Using Low-Field NMR To Infer the Physical Properties of Glassy Oligosaccharide/Water Mixtures

Kasia Aeberhardt, Quang D. Bui, and Valéry Normand*

FIRMENICH S.A., 7 rue de la Bergère, 1217 Meyrin 2 Geneva, Switzerland

Received November 3, 2006; Revised Manuscript Received December 21, 2006

Low-field NMR (LF-NMR) is usually used as an analytical technique, for instance, to determine water and oil contents. For this application, no attempt is made to understand the physical origin of the data. Here we build a physical model to explain the five fit parameters of the conventional free induction decay (FID) for glassy oligosaccharide/water mixtures. The amplitudes of the signals from low-mobility and high-mobility protons correspond to the density of oligosaccharide protons and water protons, respectively. The relaxation time of the high-mobility protons is described using a statistical model for the probability that oligosaccharide hydroxyl groups form multiple hydrogen bonds. The variation of energy of the hydrogen bond is calculated from the average bond distance and the average angle contribution. Applying the model to experimental data shows that hydrogen atoms screen the water oxygen atoms when two water molecules solvate a single hydroxyl group. Furthermore, the relaxation time of the oligosaccharide protons is independent of its molecular weight and the water content. Finally, inversion of the FID using the inverse Laplace transform gives the continuous spectrum of relaxation times, which is a fingerprint of the oligosaccharide.

Introduction

Understanding the relationship between structure and properties of the carrier matrices used in pharmaceutical, flavor, or fragrance encapsulation systems is key for the controlled release of active molecules. Starches and starch-derived products are an important class of carriers. Here we study highly hydrolyzed starches: "maltodextrins". These are legally defined as starch oligosaccharides with a number-average degree of polymerization greater than 5. The molecular weight of maltodextrins is conventionally defined by their dextrose equivalent (DE), which is defined as 100/(number-average degree of polymerization).

LF-NMR is useful for fast, routine determination of the hydrophobic flavor loading in carbohydrate-based delivery systems. Recently, this technique has been used for the fast determination of water and oil contents in a range of food systems.[1,2] However, this method requires a black-box calibration for both water and oil. Nevertheless, it was successfully adapted to encapsulated flavors.[3] Here we interpret the free induction decay (FID), the signal acquired after a 90° pulse, identifying the contribution of each relevant proton species, and give scientific insight into their relaxation time distributions.

The main objective of the present work is to extract enough information from the LF-NMR free induction decay to estimate the characteristic time distribution (CTD) for the proton relaxation in glassy oligosaccharide/water mixtures. We expect that the CTD is highly correlated with the mobility of active molecules "trapped" in the matrix and hence with the efficiency of encapsulation. A robust method to extract the CTD from the FID is a key first step in this direction.

Experimental Strategy

In glassy polymeric encapsulation systems most of the ^{1}H NMR signal results from the protons located within three components: oil, water, and the polymeric carrier. Differences in the mobility of the ^{1}H nuclei in the various hydrogen-containing constituents give spin−spin relaxation times (characterized by the relaxation time constant T_2) specific to each component. Usually, in LF-NMR, the fitting equation used to extract characteristic relaxation times and amplitudes is written as the sum of the contribution of the individual components. Each contribution is described by an independent exponential decay. A suitable fitting equation is given by[4]

$$I = A_1 \exp\left(-\frac{t^{n_1}}{T_{21}{}^{n_1}}\right)\frac{\sin(bt)}{bt} + \sum_{i>1} A_i \exp\left(-\frac{t^{n_i}}{T_{2i}{}^{n_i}}\right)$$

The first term describes the solid (polymer) signal and the second term the liquid (i.e., oil, water, ...) signals. In this equation, I is the signal intensity. A_1 and T_{21} are the amplitude and the spin−spin relaxation time (T_2) of the solid signal, respectively. n is an exponent that depends on the form of the relaxation time distribution: $n = 1$ for a Lorentzian distribution and $n = 2$ for a Gaussian distribution. b characterizes the decay rate of a damped oscillation (the so-called "sinc" function). A_{2i} and T_{2i} in the second term are the amplitudes and relaxation times of the exponential decays of the liquid signal. We only study polymer/water mixtures here, so only one exponential is required in the second term, and this equation can be simplified to give eq 1

$$I = A_1 \exp\left(-\frac{t^{n_1}}{T_{21}{}^{n_1}}\right)\frac{\sin(bt)}{bt} + A_2 \exp\left(-\frac{t^{n_2}}{T_{22}{}^{n_2}}\right) \qquad (1)$$

Thus, five parameters are needed to fit our data: two amplitudes, two spin−spin relaxation times, and the decay rate of the oscillating solid signal.

The monomer of hydrolyzed starch is anhydro-glucose. The oligosaccharide samples used in this study have already been characterized extensively.[5−7] The demagnetization of the oli-

* To whom correspondence should be addressed. Phone: +41 22 780 21 91. Fax: +41 22 780 27 35. E-mail: valery.normand@firmenich.com.

10.1021/bm061054p CCC: $37.00
Published on Web 02/10/2007

gosaccharide protons depends on several parameters, all related to the physical state of the molecule. Recently, it has been shown that the hydrogen-bonding properties of oligosaccharides depend on the molecular weight distribution[5,7] and rigidity[6] (characterized by a persistence length). These factors modify the mobility of the oligosaccharide protons.

Here our aim is to develop the simplest physical model predicting the LF-NMR spectrum of oligosaccharide−water mixtures. Once the variation of the parameters in eq 1 is explained in terms of the physical properties of the material, a CTD spectrum can be reconstructed using a minimum number of pertinent properties.

Materials and Methods

^{1}H NMR measurements were performed on a Resonance MARAN Ultra spectrometer equipped with a 18 mm variable-temperature probe. The fill height was 2 cm, and the magnetic field operation frequency was 23 MHz. The duration of the 90° pulse was 6.3 μs. The dead time was 17.1 μs. The measurement temperature was 27 °C. Oligosaccharide samples with three different molecular weights (2DE, 10DE, and 19DE)[5,7] were used. Samples were prepared by mixing oligosaccharide with deionized water for 3 min in a coffee grinder. This mixing time was sufficient as water sorption by oligosaccharide is rapid (results not shown). The mixed samples were poured into flat-bottom glass NMR tubes, weighed, and stored at 27 °C for several hours before measurement. FIDs were averaged over four scans with 4096 data points. The Karl Fischer method was used to determine the water content. The FIDs were normalized by the mass of the sample and then fitted to eq 1 with $n_1 = 2$ and $n_2 = 1$. Excel's Solver was used to perform a nonlinear least-squares fit of eq 1 to the FID.

Furthermore, T_{21} and b are parameters related to one another through the molecular structures and molecular arrangements (nonrandom molecular motions).[4] T_{21} is characteristic of the energy involved in the average interaction between protons (either C−H or O−H of the oligosaccharide molecules), thus forming dipoles, whereas b is characteristic of both the number of interactions and the distance between these dipoles. Then, the spin−spin relaxation time of the low-mobility signal (T_{21}) and its decay rate (b) are related to the strength of the dipolar interactions.[8] A theoretical development has led to the analogy between eq 1 and a Taylor series expansion of the FID in terms of moments M_n of the line shape function.[4] The singularity of this analogy is the definition of the second moment M_2. Equation 2 shows its form.

$$M_2 = \frac{2}{{T_{21}}^2} + \frac{1}{3} b^2 \qquad (2)$$

In eq 2, T_{21} and b are the fitting parameters determined by eq 1.

M_2 in maltose/water binary mixtures has been widely discussed in terms of glassy and rubbery states,[9] which confers to it a dimension related to the physical state of the overall sample.

Results and Discussion

The fits to eq 1 were always very accurate and representative of the experimental data points. In this study, we will not further discuss the quality of the fit or the adequacy of the form of eq 1.

Figure 1 shows some typical FIDs for glassy mixtures of 2DE oligosaccharide and water. The arrows show the trends in the fit parameters with increasing water content.

We observe the following trends: (1) The total intensity of the FID ($A_1 + A_2$) increases as the water fraction increases. It is proportional to the number of protons in the sample. It increases because water has a higher proton density than oligosaccharides.

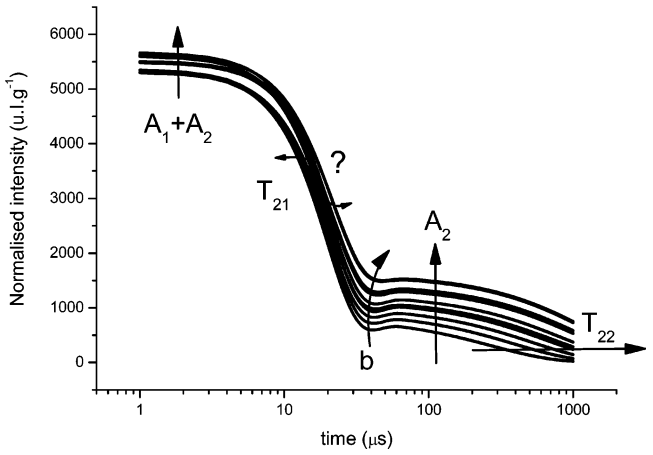

Figure 1. Typical shift behaviors in FID signals for 2DE oligosaccharide/water mixtures ranging from 10.42% to 20.26% w/w water content. The influence of the parameters of eq 1 on the shape of the FIDs for increasing water contents is described on the graph and depicted by arrows.

(2) The solid relaxation time, T_{21}, increases as the water content increases. Given that addition of water increases the mobility of the solid protons (hydroxyl protons of the oligosaccharide) presumably by increasing the proton exchange frequency, it confers a higher relaxation time on the solid proton as the water content increases. This trend is not clearly observed.

(3) The decay time b decreases with increasing water content. At very high water content, the damped oscillations, characteristic of solid behavior, disappear. The molecular motions become so important that intermolecular interactions average, giving rise to the loss of "nonrandom" structures.[4]

(4) The amplitude of the signal A_2 is related to the high-mobility proton phase concentration, whereas the relaxation time T_{22} depends on the magnitude of their mobility.[10] Field inhomogeneity, inherent to the experimental setup, influences T_{22} of highly mobile protons. The perturbation of T_{22} due to field inhomogeneity is here ignored due to the nature of the samples measured (always in the glassy state[5]). T_{22} increases when water content increases.

Measurements on mixtures made with the oligosaccharide samples with 19DE and 10DE showed identical trends.

According to eq 1, there is no interaction between solid and liquid protons. The liquid protons are due to the water molecules, and the solid protons are due to the polymer. Five parameters only describe the oligosaccharide/water FIDs: two of them are amplitudes (A_1 and A_2) and therefore related to concentrations and three are characteristic relaxation times (T_{22}, T_{21}, and b) and therefore related to energetic contributions. We now consider the physical meaning of these parameters in turn.

Amplitudes of the FID Signal (A_1 and A_2). A_1 and A_2 correspond to the amplitude of the signals from solid and liquid protons, respectively. For the solid protons these are the 10−12 different hydrogen atoms covalently bound to the oligosaccharide backbone. For the liquid protons they are the two identical hydrogen atoms of water. As in any spectrometric experiment, the signal resulting from an excitation is proportional to the amount of material being excited. In a ^{1}H NMR experiment, only the proton spins are excited. Therefore, the system of equations (eq 3) describes the signal observed at time zero.

$$\left.\begin{matrix} A_1 = k_1 n_{OH} \\ A_2 = k_2 n_H \end{matrix}\right\} \quad (3)$$

In eq 3, k_1 and k_2 are the proportionality constants and n_{OH} and n_H are the number of protons in the oligosaccharide and water, respectively. The number of protons associated with each species can be calculated using the average molecular weight and the repeating unit of the oligosaccharide. Therefore, working in moles instead of weight fraction, the number of protons is calculable for 1 g of sample of known weight fraction of water (ω_W) according to eq 4.

$$\left.\begin{matrix} n_H = \frac{2}{18}\omega_W \\ n_{OH} = \frac{(10\overline{DP_n} + 2)}{(162\overline{DP_n} + 18)}(1 - \omega_W) \end{matrix}\right\} \quad (4)$$

In eq 4, $\overline{DP_n}$ is the number-average degree of polymerization of the oligosaccharide.[5] The values of $\overline{DP_n}$ are 7, 9.7, and 46 for our 19DE, 10DE, and 2DE oligosaccharide samples, respectively.[7] Combining eqs 3 and 4 and using the experimental values of A_1 and A_2, k_1 and k_2 can be calculated. These constants are directly linked to the energy absorbed by protons during the excitation (as suggested by eq 3). They represent the average excitation state of the solid and liquid protons. We find $k_1 = 84\,730 \pm 2050$ uA·g·mol^{-1} and $k_2 = 73\,866 \pm 2277$ uA·g·mol^{-1} (here, uA stands for an arbitrary unit of amplitude). The standard deviation is around 3% for both constants. Intuitively, k_1 and k_2 should be identical as the nature of the spin excited depends only on the nature of the atom (here, a proton). The difference observed between k_1 and k_2 might be explained by the high "proton exchangeability" of the oligosaccharide hydroxyl group. Nevertheless, the fact that k_1 and k_2 have similar orders of magnitude suggests that proton exchange only makes a small contribution.

From these values it is possible to model the changes of both amplitudes with water content. We take the change in proton density with composition into account and assume that the properties of the exchangeable oligosaccharide protons are independent of the water content.

Figure 2 shows that the total amplitude increases when the amount of water increases, demonstrating an increase in the overall dipole concentration. However, in the range of water concentration screened here, the measured variability of $A_1 + A_2$ was as low as 3.5%, which allows us to consider the dipole concentration as a constant and therefore little to no influence of magnetic susceptibility modification, associated to sample formulation, on T_{21} and T_{22}. Furthermore, one can consider that the oligosaccharide molecular weight has no real influence on the results due to the small influence of the end-chain hydrogen atoms (see eq 4). The longer the chain, the lower the impact of the end-chain protons on the overall signal amplitude. Therefore, choosing the 2DE oligosaccharide as a model for all oligosaccharide molecular weights is a justified compromise.

In the current literature,[4] the ratio $A_2/(A_1 + A_2)$ is taken as directly proportional to the water content. However, the proton density was not mentioned nor was the hypothesis that the proton density was constant and independent of the water content. Here, knowing constants k_1 and k_2, the formula of the repeat unit (anhydro-glucose) and the average molecular weight of the polymer allows a reasonably good estimate of the water content. In Figures 3 and 4 the amplitude fractions are represented and compared to the predictive model just described.

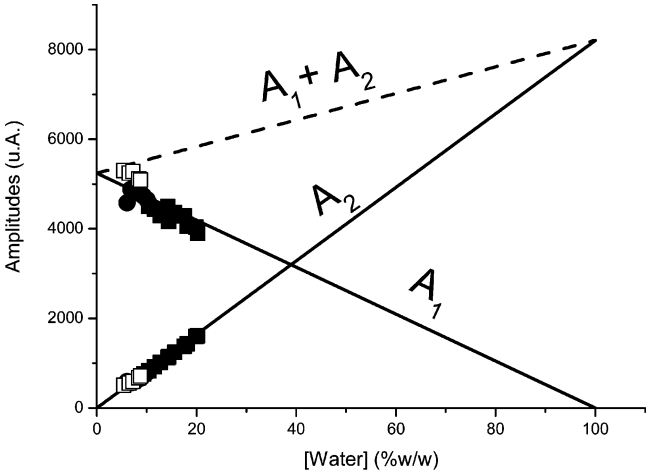

Figure 2. Theoretical evolution of A_2 and A_1 with the water content in 2DE oligosaccharide ($\overline{DP_n} = 45.96$ in eq 4). Experimental data are plotted on the graph. 2DE (solid squares), 10DE (empty squares), and 19DE (solid circles).

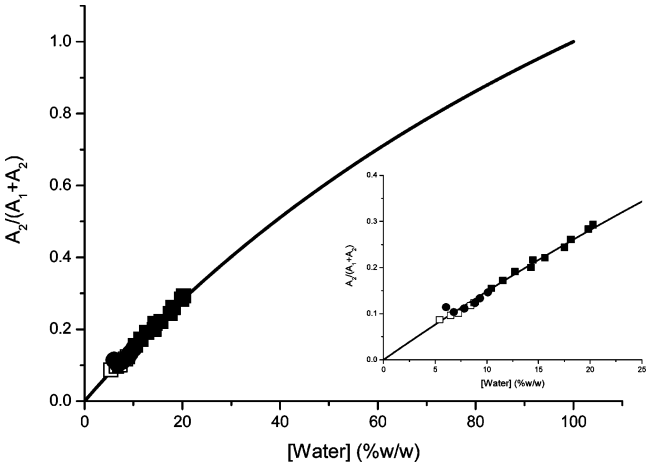

Figure 3. Correlation between the fraction of the high-mobility protons phase amplitude (A_2) over the total amplitude ($A_2 + A_1$) and water weight fraction for 2DE (solid squares), 10DE (empty squares), and 19DE (solid circles).

Satisfactory superposition is observed for both $A_1/(A_1 + A_2)$ and $A_2/(A_1 + A_2)$.

In Figures 3 and 4, a good fit is observed between the model and the experimental data. It is obvious that for large water content, water no longer acts as a plasticizer and free water is expected to be present in the solution. Also, at a given proportion of water, free sugar molecules will be detectable. Considering this, the continuous data trend should show ruptures or saturations.

Mobile Response of the FID Signal (T_{22}). The relaxation time T_{22} is supposed to be characteristic of the relaxation of water protons only, all considered as bound to the polymer by hydrogen bonds (no free water as just mentioned above). The weaker the hydrogen-bond potential energy, the freer the hydrogen atom. In other words, as the hydrogen bond stretches, the relaxation of the spin (T_{22}) occurs at much longer times. Water molecules are relatively mobile in the oligosaccharide glass due to their small size and relatively "high" diffusion coefficient.[11] Still, the diffusion coefficient is far below 10^{-8}cm^2·s^{-1} under the measurement conditions chosen and the lifetime of a hydrogen bond is approximated as longer than the transportation time of water molecule from one hydrogen-bond acceptor site to another due to the proximity of other free acceptor sites in the glass. This reduces the probability of finding

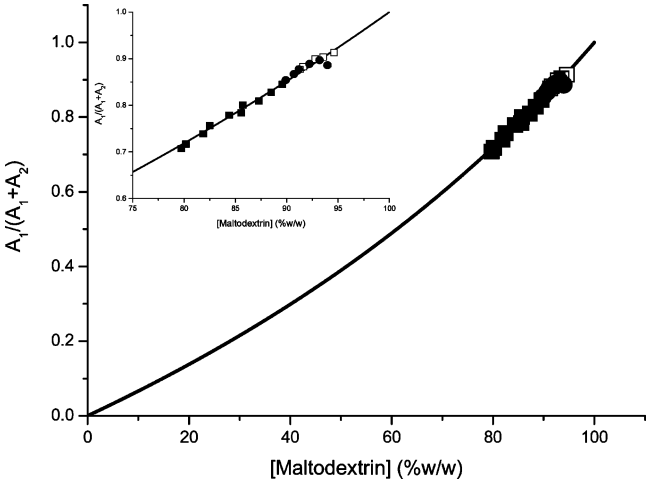

Figure 4. Correlation between the fraction of the low-mobility protons phase amplitude (A_1) over the total amplitude ($A_2 + A_1$) and oligosaccharide weight fraction for 2DE (solid squares), 10DE (empty squares), and 19DE (solid circles).

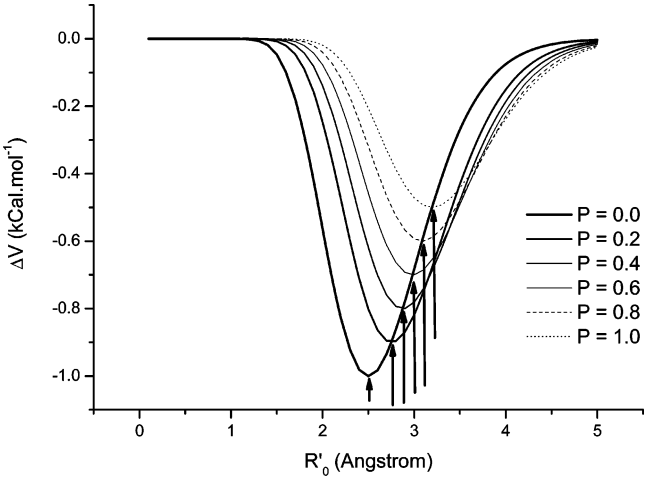

Figure 5. Reduction of the energy barrier as the probability of having two water molecules solvating one hydroxyl group increases. Determination of the equilibrium interatomic distance for the resulting bond.

free liquid water in the glassy sample and allows us to neglect the influence of diffusion on the T_{22} evolution with water concentration. As the water concentration increases, the structural properties of the glass weaken and the free volume rises, kinetically favoring exchange between the water molecules. This results in an increase in the frequency of exchange and favors the probability that more than one water molecule is bound to one hydroxyl group at a given time. Two sites are available for hydrogen-bond location. The oxygen site allows two bonds, and the hydrogen site allows a single bond with the oxygen atom of the water molecule. In the glassy state, the intrinsic negative potential of the oligosaccharide oxygen atom and the intrinsic positive potential of the water hydrogen atom can be considered to be independent of the oligosaccharide species. This is due to the assumed low water concentration, which contrasts with the zero polymer concentration already studied.[6]

It is well known that the potential energy of the hydrogen bond decreases between these two potentially oppositely charged atoms. The potential (V) of the bond is defined in eq 5.[12]

$$V = D_0\left(1 - \exp\left(-\frac{n\Delta R^2}{2R}\right)\right) \tag{5}$$

In eq 5, D_0 is the dissociation energy that can be considered as being the energetic barrier of the bond. R is the internuclear distance. ΔR is the elongation of the bond from its equilibrium position ($\Delta R = R - R_0$). R_0 is the equilibrium bond length. Finally, n is a constant related to atomic ionization.[12]

To simplify the graphical representation, eq 5 can be also expressed in the form of eq 6.

$$\Delta V = -D_0 \exp\left(-\frac{n\Delta R^2}{2R}\right) \tag{6}$$

Equation 6 is similar to eq 5. However, ΔV now represents the energetic barrier corresponding to dissociation of the bond.

Hydrogen-bond stretching is caused by competition for hydroxyl groups. The probability of finding more than one water molecule bound to a hydroxyl is far from zero as soon as more than one water molecule enters the system. As reported in the literature,[6] the maximum number of water molecules per hydroxyl group is close to 2 and independent of the oligosaccharide molecular weight. This has been measured by high-resolution ultrasonic wave spectroscopy when there is an excess of water. If more than one water molecule bonds to one hydroxyl group, there is equivalence of bond energy (water molecules are indistinguishable). The energy per bond (D') is the available energy (D_0 as in eqs 5 and 6) affected by the probability (P) of the presence of more than one molecule, reducing the strength of each bond. The potential properties (eq 6) allow the determination of the internuclear distance (R' and R'_0 in equilibrium condition) of a single hydrogen atom forming the resulting unique bond. This is possible when equating D' and ΔV (see eq 7)

$$\left\{\begin{aligned} D' &= D_0\left(1 - \frac{P}{2}\right) \\ D' &= -D_0 \exp\left(-\frac{n\Delta R'^2}{2R'}\right) \end{aligned}\right\} \tag{7}$$

Solving eq 7 gives a value of R' that is the average equilibrium distance at which a single water hydrogen atom is located from the hydroxyl, taking into account the energy loss of the bond when the probability of finding more than one water molecule increases. Figure 5 illustrates this point.

Figure 5 shows the theoretical evolution of the energy barrier, which decreases with increasing solvation of the oligosaccharide.

If oxygen and hydrogen atoms of the hydroxyl group generate hydrogen bonds, two proton motions will influence the characteristics of the FID. Those motions should be revealed in LF-NMR by two individual relaxation times, unless the diffusion of water molecules in the glassy matrix allows for water molecule exchange on a time scale much shorter than the measured T_{22}. Measurements of the diffusion coefficient of water in oligosaccharide/water systems have been reported already for these sample materials.[11,13] These show a dramatic decrease of this coefficient when the water concentration decreases. Under the concentration conditions tested here, a diffusion coefficient of the order of 2×10^{-9} cm^2 s^{-1} is extrapolated. This is in agreement with a rate of water diffusion which is too small.[10] Another view of the fully hydrated system considers the oxygen of the hydroxyl group as the unique site for hydrogen-bond generation. This system is considered here. From an electrostatic viewpoint, the two water molecules forming the two hydrogen bonds are shifted angularly from the pure linearity of the atoms forming the hydrogen bond of higher energy (linearity $O-H_w\cdots O_m$ (subscript "w" for water and "m" for oligosaccharide)). This is due to the repulsive interaction of the water

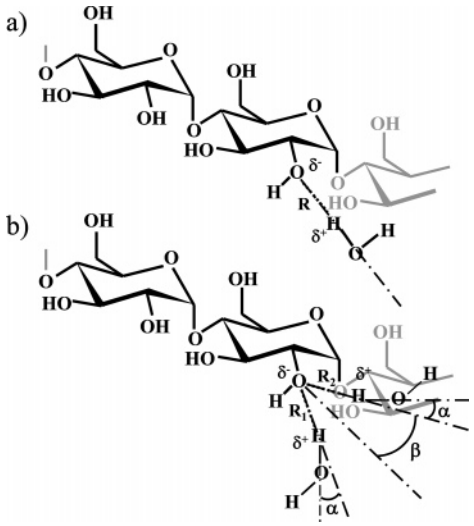

Figure 6. Schematic representation of the hydration of oligosaccharide. Constraints generated by competition between electrostatic forces.

oxygen atoms. Figure 6 shows the variation of angle proposed when more than one water molecule solvates one hydroxyl group. The angular shift (α in Figure 6) is due to electrostatic oxygen−oxygen repellence.[12]

Such angular shifts have already been extensively studied.[12,14,15] Moulton and Kromhout derived a potential function of the hydrogen bond, which describes the distortion of bond angles from the normal bond direction. They obtained eq 8 from quantum mechanical theories.

$$V = D_0\left(1 - \exp\left(-\frac{n\Delta R^2}{2R}\right)\cos^2\alpha\right) \tag{8}$$

In eq 8, notations are identical to those used in eq 5 and α is the angle between the O−H bond and the nonshifted ideal O−H bond direction (see Figure 6b). As previously stated, the energy barrier is also well described using eq 9.

$$\Delta V = -D_0 \exp\left(-\frac{n\Delta R^2}{2R}\right)\cos^2\alpha \tag{9}$$

According to eq 9, the equilibrium potential (minimum on the potential function) is increased when α increases. Again, this is similar to the effect of P on the energy barrier.

If it is stated that P is responsible for the bending of the bond, R'_0 (Figure 5) and α (Figure 7) have cumulative effects. To demonstrate this effect, a maximum angle ($\alpha = 50°$ if $P = 1.0$) is arbitrarily defined and a linear relationship between P and α is also considered. Then an estimation of the cumulative effect can be derived. Results are shown in Figure 8 (eq 7 was inserted into eq 9).

Depending on the maximum angle value and the probability that hydroxyl groups are solvated by one or two water molecules on average at any given time, the energy associated with one hydrogen bond should be dependent on the number of water molecules per hydroxyl group. However, the missing factor is the function relating n_H/n_{OH} to the probability to find two water molecules bonded to one hydroxyl. This is accessible using complex extended statistical theories.[9,16,17] A simpler way to reach identical information is to consider conventional probability theories. This method is easier to explain. Therefore, this simplified explanation is preferred.

For illustration, a system composed of a single-chain polymer containing a not too large but constant number of hydrogen-

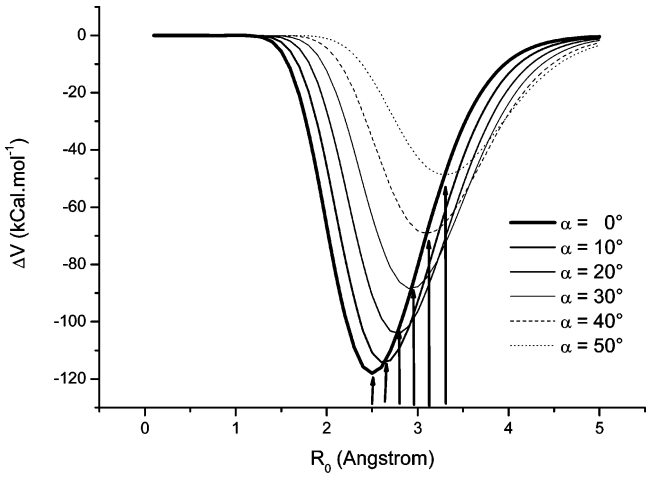

Figure 7. Illustration of eq 11 with parameters reported in the literature[12] and angle values of 0°, 10°, 20°, 30°, 40°, and 50° and $R_0 = 2.5$Å.

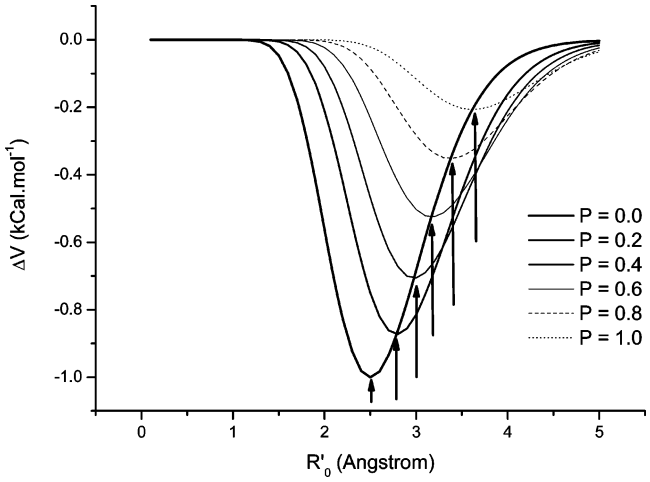

Figure 8. Evolution of the potential combining the probability function P and α, with $\alpha = 50°$ when $P = 1$ as an example.

bond acceptor sites (n_A) and a variable number of hydrogen-bond donor molecules (n_D) is considered. The acceptor sites can accept 0, 1, or 2 donor molecules until saturation is reached (2 donor molecules per acceptor site), and n_D thus varies between 0 and $2n_A$. The ratio n_D/n_A is identical to the ratio n_H/n_{OH} in the oligosaccharide case. An example is given for a "polymer" having three acceptor sites in Figure 9, where the number of single bonds (n_1) and double bonds (n_2) together with the probability P are explained.

For a given ratio n_D/n_A between 0 and 2, the number of possibilities that the acceptor sites are linked to one donor molecule only (n_1) or two donor molecules (n_2) is defined by eqs 10a and 10b, respectively.

$$n_1 = \sum_{j=0}^{n_D/2} (n_D - 2j)\left[\frac{(n_A - j)!}{(n_A - n_D + j)!(n_D - 2j)!}\right]\left[\frac{n_A!}{(n_A - j)!j!}\right] \tag{10a}$$

$$n_2 = \sum_{j=0}^{n_D/2} 2j\left[\frac{(n_A - j)!}{(n_A - n_D + j)!(n_D - 2j)!}\right]\left[\frac{n_A!}{(n_A - j)!j!}\right] \tag{10b}$$

The characteristic of the average donor molecule has intermediate properties between the properties of population 1 and population 2 if the properties are different. P as defined in eq

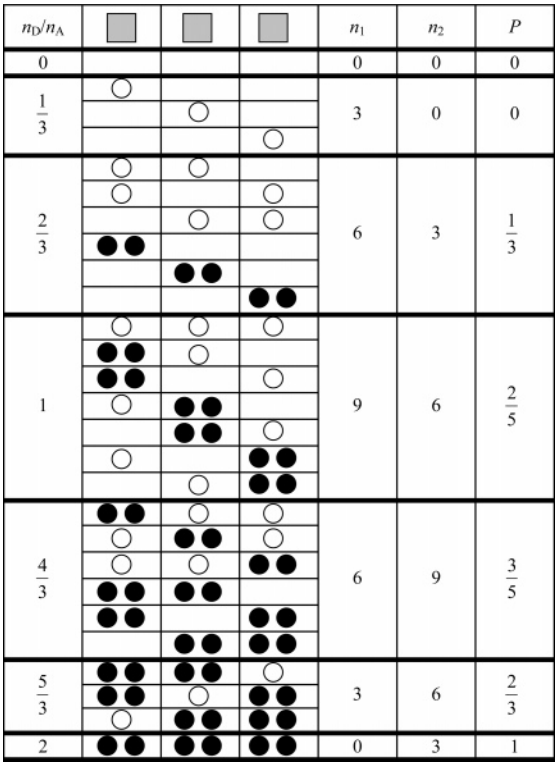

Figure 9. Probability of the presence of two bonds (plain circles) on available acceptor sites (grey squares) for a system formed by one polymer chain containing three acceptor sites and an increasing number of donor sites. Empty circles stand for single donor−acceptor bonds.

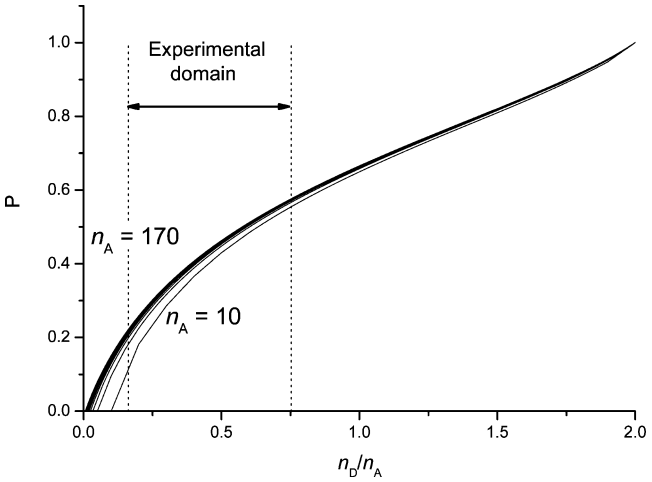

Figure 10. Determination of the probability for two water molecules to be linked to one hydroxyl for all water molar fractions. The lines correspond to the calculations for increasing number of acceptor sites between 10 and 170 with steps of 10.

7 is now expressed directly as a function of n_A and n_D by eq 11 for this model acceptor/donor system.

$$P_{(nD/nA)} = \frac{n_{2(n_D/n_A)}}{n_{1(n_D/n_A)} + n_{2(n_D/n_A)}} \quad (11)$$

A representation of the variation of P with n_D/n_A for a single polymer chain characterized by n_A comprised between 10 and 170 (limit reached by a conventional personal computer using double precision variables) is presented in Figure 10.

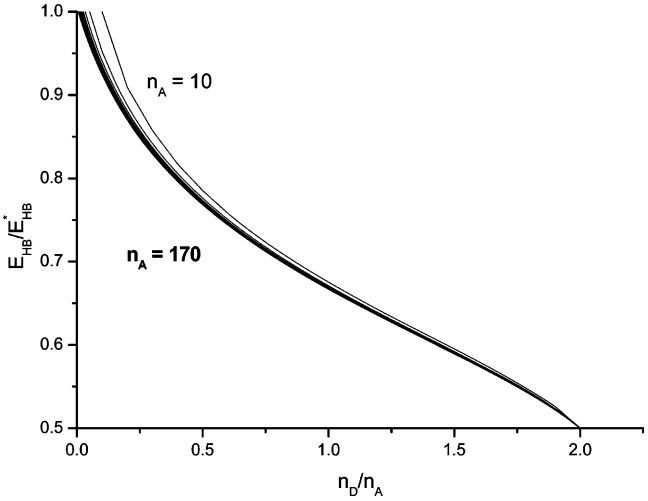

Figure 11. Evolution of the energy of the hydrogen bond with the ratio donor/acceptor. The lines correspond to the calculations for increasing number of acceptor sites between 10 and 170 with a step of 10.

The energy (E_{HB}) that characterizes the average acceptor/donor bond is then calculated using eq 12 for a single polymer chain characterized by n_A with values between 10 and 170.

$$E_{HB} = \left(1 - \frac{P_{(nD/nA)}}{2}\right) E^*_{HB} \quad (12)$$

In eq 12, E^*_{HB} represents the hydrogen-bond energy when all the existing hydrogen bonds involve one donor only per acceptor site. The results of the simulation are presented in Figure 11.

According to Figure 11 the decrease of energy of the hydrogen bond is not linear with n_D/n_A. Remarkably, hidden information is revealed. The system can be seen as one single polymer chain and characterized by the number of acceptor sites. Therefore, E_{HB} is independent of the distribution of chain lengths with identical structural units (here poly maltose). All T_{22} data linked to some extent to E_{HB} should be on the same curve.

However, for direct comparison between the model and the experimental data, P should be calculated for n_D/n_A corresponding to sample conditions. A fourth degree polynomial function fits perfectly ($R^2 = 0.9995$) the calculated data (see eq 13).

$$P = q_4\left(\frac{n_D}{n_A}\right)^4 + q_3\left(\frac{n_D}{n_A}\right)^3 + q_2\left(\frac{n_D}{n_A}\right)^2 + q_1\left(\frac{n_D}{n_A}\right) + q_0 \quad (13)$$

Determination of P is now possible for experimental values of n_H/n_{OH}, as shown in Figure 12.

The strategy now is to determine the angle α, which best characterizes the system when two water molecules solvate a single hydroxyl group. First, eqs 8 and 9 should be rewritten as eqs 14 and 15 to account for the two water molecules

$$V = D_0\left(1 - \frac{P}{2}\right)\left(1 - \exp\left(-\frac{n\Delta R^2}{2R}\right)\cos^2(2P\alpha)\right) \quad (14)$$

$$\Delta V = -D_0\left(1 - \frac{P}{2}\right)\exp\left(-\frac{n\Delta R^2}{2R}\right)\cos^2(2P\alpha) \quad (15)$$

The maximum amplitude of the potential (when excluding the exponential function) should then be linearly correlated to the resonance energy of water hydrogen atom. This energy is proportional to $1/T_{22}$ (see eq 16).

$$E^*_{HB} \propto \Delta V \equiv \frac{1}{T_{22}\left(\frac{n_H}{n_{OH}}\right)} \propto D_0\left(1 - \frac{P\left(\frac{n_H}{n_{OH}}\right)}{2}\right)\cos^2\left(2P\left(\frac{n_H}{n_{OH}}\right)\alpha\right) \quad (16)$$

Using the "Excel solver" function tool, the best correlation obtained for α approximately equals 90° (see Figure 13).

The results presented in Figure 13 are in favor of the interpretation that, in the case of solvation by two water molecules, the oxygen atoms of the two water molecules are fully screened by the two hydrogen atoms forming the bonds. Accordingly, T_{22} can be evaluated knowing the composition of the system (n_H/n_{OH}). However, this rigorous treatment fails due to the $1/T_2$ dependence when the water content increases. Furthermore, it is not straightforward to apply it to all measurements unless the relationship between P and n_H/n_{OH} is empirically modeled. A direct linear relationship between T_{22} and $(n_H/n_{OH})^2$ can also be applied but is scientifically unfounded.

A representation of T_{22} as a function of the square of the molar fraction of water over the molar fraction of hydroxyl group (see eq 4) is given in Figure 14.

Again, the quantities represented in Figures 13 and 14 are independent of the oligosaccharide species. According to the regression equation (see Figure 14 caption), for zero water weight fraction, T_{22} has no meaning. This statement is logical: for zero water molecules, the oligosaccharide glassy properties are extreme and all the relaxation processes are extremely rapid.

Low-Mobility Protons Response of the FID Signal (T_{21} and b). The signal of the low-mobility protons response is generally treated as a whole using the properties of the fitting equation as explained earlier and eq 2 is used to determine the value of the second moment of the response.

(1) M_2 evolves linearly with the quantity $T - T_G$ for various carbohydrate materials and mixtures thereof in the glassy state.[4,9,18] In the present study, T is constant (measurement temperature = 27 °C) and T_G varies with the water content. T_G is determined through Couchman's classical model[19] that has been successfully applied to those oligosaccharide samples mixed with water in a similar range of concentrations.[5] The representation of M_2 as a function of $T - T_G$ is presented in Figure 15 for the three oligosaccharide species studied.

The slope of M_2 as a function of $T - T_G$ evolves with the type of the oligosaccharide. Furthermore, it is function of the number-average molecular weight, and eq 17 allows evaluation of the second moment with respect to water content.

$$M_2 = K(M_n)^k\left(T - T_{G\left(\frac{nH}{nOH}\right)}\right) + C(M_n) + c \quad (17)$$

Here, K, k, C, and c are empirical constants, and M_n and T_G are the number-average molecular weight of the oligosaccharide sample and the glass transition of this particular sample at a given water content, respectively. The number of empirical parameters of the model equation is too high to propose a robust theoretical explanation. Therefore, these constants will not be challenged. The values derived from the appropriated fits are -2.44×10^6 s^{-2}, 0.215, -1.02×10^5 mol·g^{-1}·s^{-2}, and 5.50×10^9 s^{-2} for K, k, C, and c respectively.

Only knowing M_2 does not allow characterization of the low-mobility proton relaxation signal. Another parameter (T_{21} or b) is needed.

(2) T_{21} is very short when compared to the dead time inherent to the setup. Of course, this will increase the error made in the determination of this parameter. First, T_{21} varies from 28.7 to 31.5 μs for different oligosaccharides and at various water contents. This means that the low-mobility protons are strongly immobilized by interactions with neighboring dipoles.[4] Second, no real trend is noticed when the water content varies (T_{21} varies randomly with the water content, the sensitivity of the experimental setup is reached) giving T_{21} a large robustness. Therefore, it is suggested that T_{21} can easily be taken as a general constant independent of the oligosaccharide species. The average value is 30.06 ± 0.81 μs, taking into account all the experiments performed.

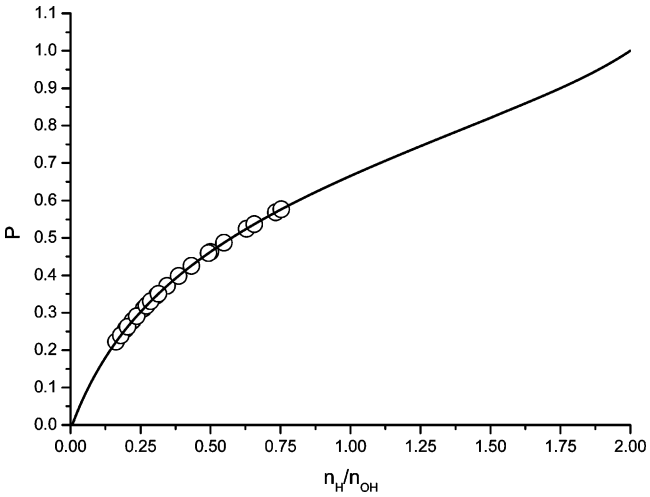

Figure 12. Graphical determination by interpolation of the probability for two water molecules to be linked to one hydroxyl site for experimental values of n_H/n_{OH}. The parameters of the fit are q_0 = 0.021458, q_1 = 1.354807, q_2 = −1.19638, q_3 = 0.588324, and q_4 = −0.10406.

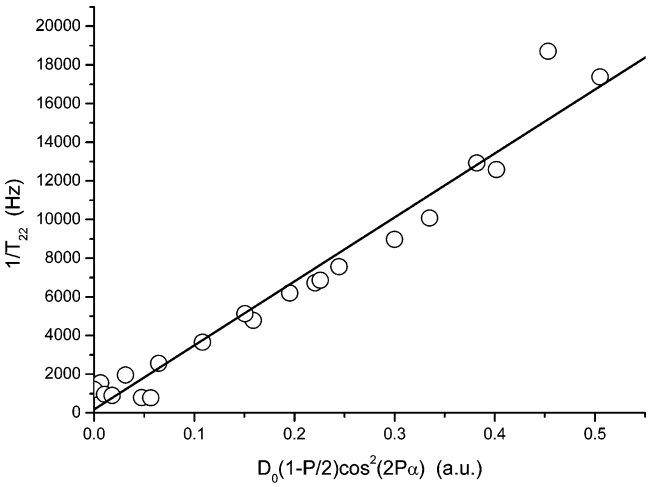

Figure 13. Best correlation between experimental resonance data and calculated energy of the average hydrogen bond for all experimentally tested water fractions. R^2 = 0.9588 for α = 92.25°. The slope is 33 659 for D_0 = 1 (a.u. stands for arbitrary unit).

(3) b is used commonly as an empirical fitting parameter.[9] In this work, it is defined as a characteristic of a spring (spin over-relaxation) and therefore representative of the material mechanical state. It decreases as the water content increases due to the increase of motion in the system.[4] It has been demonstrated that, in carbohydrate matrices, the coefficients of expansion are constant in the glassy (α_G) and rubbery (α_R) states. In extruded starches, α_R is 2.3 times α_G[20]. Starting in the glassy state, as long as the glass transition is not reached, the specific volume increases linearly with the water content. As shown earlier, T_{21} can be approximated to be constant. According to eq 4, M_2 evolves linearly with b^2 (results not shown). The regression coefficient (R^2) is 0.9831 when all the samples are

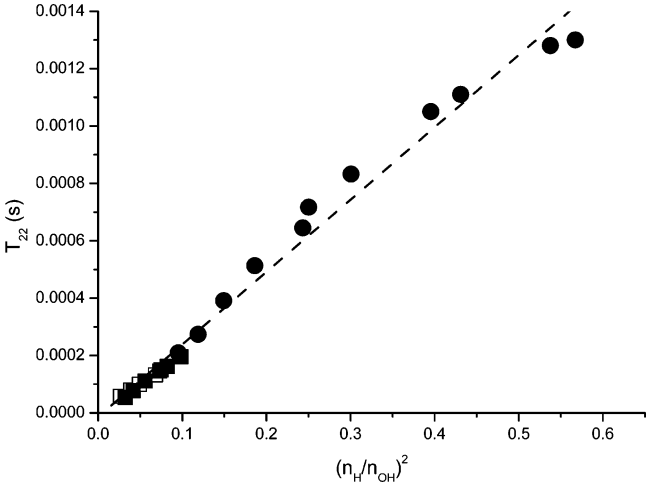

Figure 14. Correlation between the high-mobility proton phase characteristic relaxation time (T_{22}) and the square of the number of water molecules per hydroxyl group for 2DE (solid squares), 10DE (empty squares), and 19DE (solid circles). The slope is 2.45×10^{-3}. The regression passes through zero, and R^2 is 0.993.

considered. The slope is $0.3125 \pm 8.3 \times 10^{-3}$ (close to 1/3 as expected from eq 2), and the average T_{21} as calculated from the intercept (see eq 2) is $28.31 \pm 0.16\ \mu$s. This important result demonstrates that under the experimental conditions investigated here, T_{21} is not affected by the state of the system. Only b is sensitive to changes in the structure induced by water addition. T_{21} is a constant of the polymer independent of its molecular weight and characterizes the solid state whatever the mechanical properties are. The loss of cohesive energy associated with the decrease in b evolves with the water content. Concomitantly, its influence on the relaxation spectrum disappears. The limit of the *sinc* function when b tends toward zero is unity. It is worth noting that b is expected to evolve differently when the system undergoes the glass transition.

According to eqs 2 and 17, b is linked to the part of eq 17 sensitive to the water content ($T - T_G$) and to the molecular weight, whereas T_{21} accounts for the independent constant (when $T = T_G$).

Thus, the following equations are proposed

$$\left\{\begin{aligned} T_{21} &= \sqrt{\frac{2}{c'}} = 30.06\ \mu\text{s} \\ b &= \sqrt{3\left(K(M_n)k\left[T - T_G\left(\frac{n_H}{n_{OH}}\right)\right] + C(M_n) + (c - c')\right)} \end{aligned}\right\} \tag{18}$$

b is then accessible knowing M_n and the ratio of water per hydroxyl (n_H/n_{OH}).

All the relevant parameters have been explained in terms of their physical meanings. Therefore, reconstruction of a series of model FIDs is possible knowing the water content, the number-average molecular weight of the oligosaccharide, and its T_G for zero water content. The final objective is to understand the evolution of the relaxation time distribution associated with the relaxation spectrum.

Characteristic Time Distributions (CTD). Extraction of characteristic time distributions (CTD) from relaxation experiments is a widely used methodology in rheology and LF-NMR spectroscopy. From the CTD numerous physical properties are understood and derived.[21] This is the fingerprint of the product analyzed. In rheology it is obtained from the inversion of the mechanical relaxation spectrum. The FID has similarities with

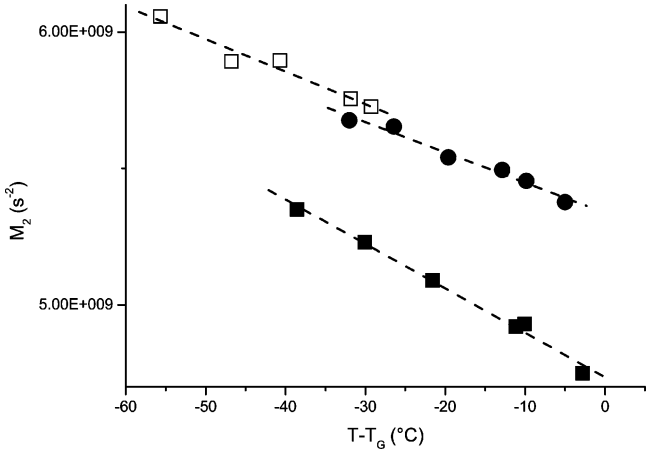

Figure 15. Classical representation of M_2 as a function of the glassy-state properties ($T - T_G$) for three oligosaccharides (2DE, filled squares; 10DE, open squares; 19DE, filled circles).

mechanical relaxation spectra. Therefore, CTD allows determination of structure/property relationships. Also, small changes in the composition cause more visible changes in the CTD than the FID itself.

The simplest way of extracting the characteristic time function from a relaxation curve is the Schwarzl−Staverman[22] procedure, commonly used as an alternative to the theoretical inverse Laplace transform. Once the influence of b on the solid-state relaxation is removed from the FID (see eq 1), which defines the partial signal intensity I^*, the corrected FID becomes simply a sum of exponential functions and I^* can be rewritten as eq 19, a continuous spectrum of relaxation

$$\left\{\begin{aligned} I^*(t) &= A_1 \exp\left(-\frac{t^2}{{T_{21}}^2}\right) + A_2 \exp\left(-\frac{t}{T_{22}}\right) \\ I^*(t) &\equiv \int_{-\infty}^{+\infty} F_S(\tau) \exp\left(-\frac{t^2}{\tau^2}\right) \mathrm{d}\ln\tau + \\ &\quad \int_{-\infty}^{+\infty} F_M(\tau) \exp\left(-\frac{t}{\tau}\right) \mathrm{d}\ln\tau \end{aligned}\right\} \tag{19}$$

In eq 19, $F_S(\tau)$ and $F_M(\tau)$ are the relaxation time distributions for low- and high-mobility protons, respectively, and extracted from the experimental FID using the simple first-order transformation,[22] as used in rheology from Alfrey and Doty's rule.[23]

$$F(\tau) \cong -\left.\frac{\mathrm{d}I^*(t)}{\mathrm{d}\ln(t)}\right|_{t=\tau} \tag{20}$$

In the present work, only one species forms the high-mobility protons signal (water). Modeling the FID presented in Figure 1 and removing the part of the signal due to the low-mobility protons allows representation of the characteristic time distribution under various experimental conditions for the high-mobility protons. Evolution of the characteristic time distribution under the conditions of Figure 1 with gradual increase in water content is shown in Figure 16.

Figure 16 shows that as the water content increases, the amplitude of the signal from the low-mobility protons decreases whereas the amplitude of the signal from the high-mobility protons increases.

The continuous distribution of characteristic times is the fingerprint of the product analyzed. According to this study, only three parameters are necessary to reconstruct the FID of a simple glass composed of oligosaccharide and water: The molecular weight of the oligosaccharide, water content, and

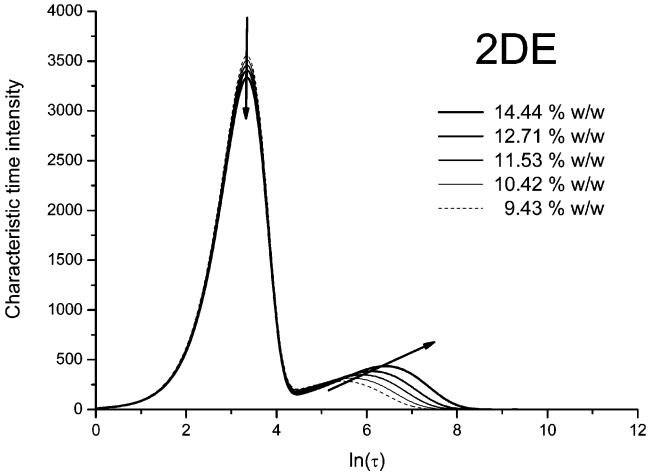

Figure 16. Modification of the characteristic time distribution with increasing water content. Curves are calculated from the reconstructed FID using the theories developed in this work.

temperature. This work leads naturally to an opportunity to assess the effect of other plasticizers on the full spectrum together with the aim of measuring their concentrations.

Conclusion

A fundamental approach to the LF-NMR FID fitting patterns of glassy oligosaccharide/water mixtures led to the physical understanding of all the empirically used parameters. FID can now be produced with very good accuracy knowing only three pieces of information: the molecular weight of the oligosaccharide, water content, and temperature at which the measurement is performed. Among the fundamental results found, the variation of the hydrogen-bond energy is probably the most interesting, despite the fact that its use in this work is limited.

The continuous distribution of characteristic times of the species present in the system is obtainable through classical rheological theories. This will certainly be valuable for further studies on the rubbery state of the same system and characterization of plasticizing molecules other than water for quantification purposes. In the future, a reverse methodology will be very useful to characterize unknown samples.

Acknowledgment. Drs. H. Sommer, I. Farhat, and A. Parker are greatly acknowledged for fruitful and constructive discussions.

References and Notes

(1) Rubel, G. Simultaneous determination of oil and water contents in different oilseeds by pulsed nuclear magnetic resonance. *JAOCS* **1994**, *71* (10), 1057−1062.

(2) Brosio, E.; Conti, F.; Di Nola, A.; Scorano, O.; Balestrieri, F. Simultaneous determination of oil and water content in olive husk by pulsed low resolution nuclear magnetic resonance. *J. Food Technol.* **1981**, *16*, 629−636.

(3) Todt, H.; Burk, W.; Guthausen, G.; Guthausen, A.; Kamlowski, A.; Schmalbein, D. Quality control with time-domain NMR. *Eur. J. Lipid Sci. Technol.* **2001**, *103*, 835−840.

(4) Derbyshire, W.; van den Bosch, M.; van Dusschoten, D.; McNaughtan, W.; Farhat, I. A.; Hemminga, M. A.; Mitchell, J. R. Fitting of the beat pattern observed in NMR free-induction decay signals of concentrated carbohydrate-water solutions. *J. Magn. Reson.* **2004**, *168*, 278−283.

(5) Avaltroni, F.; Bouquerand, P.-E.; Normand, V. Oligosaccharide molecular weight distribution influence on the glass transition temperature and viscosity in aqueous solutions. *Carbohydr. Polym.* **2004**, *58* (3), 323−334.

(6) Aeberhardt, K.; de Saint Laumer, J.-Y.; Bouquerand, P.-E.; Normand, V. Ultrasonic study of sugars oligomers and oligosaccharide solutions: Persistence length and radius of gyration. *Int. J. Biol. Macromol.* **2005**, *36* (5), 275−282.

(7) Normand, V.; Avaltroni, F.; Bouquerand, P.-E. Mathematical discretisation of Size-Exclusion-Chromatograms applied to commercial corn oligosaccharides, *J. Chromatogr. Sci.* **2006**, *44* (2), 91−95.

(8) Abragam A. *The principle of Nuclear Magnetism*; Clarendon Press: Oxford, 1961.

(9) Van den Dries, I. J.; van Duchossen, D.; Hemminga, M. A. Mobility of maltose-water glasses studied with ^{1}H NMR. *J. Phys. Chem. B.* **1998**, *102*, 10483−10489.

(10) Radosta, S.; Schierbaum, F. Polymer-water interaction of oligosaccharides, Part II: NMR study of bound water in liquid oligosaccharide-water systems. *Starch/Stärke* **1989**, *41* (11), 428−430.

(11) Bouquerand, P. E.; Maio, S.; Atkins, D.; Singleton S.; Normand, V. Swelling and erosion affecting flavor release from glassy particles in water, *AIChE J.* **2004**, *50* (12), 3257−3270.

(12) Lippincott, E. R. Deviation of an intermolecular potential function from a quantum mechanical model. *J. Chem. Phys.* **1955**, *23*, 603.

(13) Ouali, L.; Leon, G.; Normand, V.; Benczédi, D.; Johnsen, H.; Dyrli, A.; Schmid, R. Mechanism of Romascone release from hydrolysed vinyl acetate nano-particles: thermogravimetric method. *Polym. Adv. Technol.* **2006**, *17* (1), 45−52.

(14) Schroeder, R.; Lippincott, E. R. Potential function model of hydrogen bonds. *J. Phys. Chem.* **1957**, *61*, 921−928.

(15) Moulton, W. G.; Kromhout, R. A. Nuclear Magnetic Resonance: Structure of the Amino Group. II. *J. Chem. Phys.* **1956**, *25* (1), 34−37.

(16) Veytsman, B. Thermodynamics of hydrogen-bonded fluids: effects of bond cooperativity. *J. Phys. Chem.* **1993**, *97*, 7144−7146.

(17) Veytsman, B. Equation of state for hydrogen-bonded systems. *J. Phys. Chem. B* **1998**, *102*, 7515−7517.

(18) Kumagai, H.; McNaughtan, W.; Farhat, I. A.; Mitchell, J. R. The infuence of carrageenan on the molecular mobility in low moisture amorphous sugars. *Carbohydr. Polym.* **2002**, *48*, 341−349.

(19) Couchman, P. R. Compositional variation of glass transition temperature. 2. Application of the thermodynamic theory to compatible polymer blends. *Macromolecules* **1978**, *11* (6), 1156−1161.

(20) Benczédi, D.; Tomka, I.; Escher, F. Thermodynamics of amorphous starch-water systems. 1. Volume fluctuations. *Macromolecules* **1998**, *31* (9), 3055−3061.

(21) Schwarzl, F. R. *Polymermechanik*; Springer-Verlag: Berlin, Heidelberg, and New York, 1990; p 338.

(22) Schwarzl, F. R.; Staverman, A. J. Higher approximation methods for the relaxation spectrum from static and dynamic measurements of visco-elastic materials. *Appl. Sci. Res.* **1953**, *A4*, 127−141.

(23) Alfrey, T.; Doty, P. The methods of specifying the properties of viscoelastic materials. *J. Appl. Phys.* **1945**, *16*, 700−713.

BM061054P